

Brownian particles in supramolecular polymer solutionsJ. van der Gucht,^{1,2,*} N. A. M. Besseling,¹ W. Knoben,¹ L. Bouteiller,³ and M. A. Cohen Stuart¹¹Laboratory of Physical Chemistry and Colloid Science, Wageningen University, P.O. Box 8038, 6700 EK Wageningen, The Netherlands²Dutch Polymer Institute, Eindhoven, The Netherlands³Université Pierre et Marie Curie–CNRS, UMR 7610: Chimie des Polymères, 4 place Jussieu, 75252, Paris cedex 05, France

(Received 6 January 2003; published 19 May 2003)

The Brownian motion of colloidal particles embedded in solutions of hydrogen-bonded supramolecular polymers has been studied using dynamic light scattering. At short times, the motion of the probe particles is diffusive with a diffusion coefficient equal to that in pure solvent. At intermediate time scales the particles are slowed down as a result of trapping in elastic cages formed by the polymer chains, while at longer times the motion is diffusive again, but with a much smaller diffusion coefficient. The influence of particle size and polymer concentration was investigated. The experimental data are compared to a theoretical expression for the mean-square displacement of an embedded particle in a viscoelastic medium, in which the solvent is explicitly taken into account. Differences between the friction and elastic forces experienced by the particle and the macroscopic viscosity and elasticity are explained by the inhomogeneity of the medium on the length scale of the particle size.

DOI: 10.1103/PhysRevE.67.051106

PACS number(s): 05.40.Jc, 81.16.Fg, 83.10.Pp, 83.85.Ei

I. INTRODUCTION

The Brownian motion of colloidal particles in complex media is a subject of fundamental interest in statistical physics and is also relevant for many technological applications and biological processes. Moreover, by monitoring the thermal fluctuations of dispersed probe particles, information can be obtained about the structure and dynamics of the medium on a microscopic level [1]. Various optical techniques, such as dynamic light scattering and diffusing wave spectroscopy, have been employed to measure the Brownian motion of dispersed particles in, for example, polymer solutions [2–6], gels [7–10], solutions of protein filaments [11,12], concentrated colloidal systems [13–15], and micellar solutions [16–18].

In this paper, we study Brownian motion of probe particles dispersed in solutions of supramolecular polymers. These are linear chains of small molecules held together by noncovalent, reversible bonds [19–21]. They are also referred to as “equilibrium polymers” or “living polymers,” and have much in common with other living polymers, such as wormlike micelles [22,23]. Supramolecular polymers not only reproduce many of the properties of traditional polymers but also introduce distinct features, because they can break and recombine on experimental time scales. The molecular weight distribution of supramolecular polymers is not fixed but responds to variable conditions such as the monomer concentration and the temperature. The average length increases with increasing concentration and decreasing temperature [22,23].

One of us recently reported the synthesis of self-assembling monomers based on urea groups [24,25]. These monomers form long, semiflexible polymer chains in apolar solvents as a result of multiple hydrogen bonding between the monomers. The reversible polymerization was investi-

gated using viscosimetry, infrared spectroscopy, small-angle neutron scattering, and rheology. At high enough concentration, the chains entangle and form highly viscoelastic solutions.

We study Brownian motion of colloidal particles in solutions of these supramolecular chains using dynamic light scattering. We show that the motion is governed by the solvent viscosity at short times, while at longer times the particles are slowed down by the viscoelasticity of the polymer network. At present, the short-time behavior of embedded probe particles in a polymer solution gives rise to a debate: most authors find subdiffusive behavior at short times, which is usually ascribed to the viscoelasticity of the polymer network [7,8,11,16]. Recently, however, Bellour *et al.* argued that the short-time dynamics should be diffusive and governed by the solvent viscosity [18]. Although the latter point was not clearly observed in their experiments, they could fit their data with an expression that leads to diffusive motion at short times. The experiments described in the present paper do clearly show a diffusive motion at short times, which is independent of the polymer concentration. Hence the friction due to the solvent dominates the elastic forces exerted by the polymer chains at these time scales. In Sec. II, we show how the solvent friction can be included in the Langevin description of a Brownian particle in a viscoelastic medium. We derive an expression for the mean-square displacement of a particle in a polymer solution, which adequately describes the short-time diffusive motion. At longer times it corresponds to the motion of a particle in a Maxwellian viscoelastic fluid. Furthermore, we discuss the connection between the mean-square displacement of the particles and the macroscopic viscosity and elasticity of the medium. The model predictions are compared to the experimental results in Sec. IV for various polymer concentrations and particle sizes. We find significant differences between the local viscous and elastic forces experienced by the moving particles and the macroscopic viscosity and elasticity of the polymer solutions. We discuss these differences in detail, and relate them

*Electronic address: jasper.vandergucht@wur.nl

to inhomogeneity of the medium on length scales smaller than the mesh size of the polymer network.

II. THEORETICAL BACKGROUND

The Brownian motion of a particle is characterized by its mean-square displacement $\langle \Delta r^2(t) \rangle$. In the case of free diffusion this is a linear function of time:

$$\langle \Delta r^2(t) \rangle = 6Dt, \quad (1)$$

where D is the diffusion coefficient. For a spherical particle with hydrodynamic radius R in a solvent with viscosity η , the diffusion coefficient is given by the Stokes-Einstein relation:

$$D = \frac{kT}{\zeta}, \quad (2)$$

where k is the Boltzmann constant, T is the temperature, and ζ is the Stokes' friction coefficient, under no-slip conditions given by

$$\zeta = 6\pi\eta R. \quad (3)$$

The Stokes-Einstein relation is valid for particles diffusing in a continuous, nonelastic Newtonian medium. Many complex media, however, such as semidilute polymer solutions, are viscoelastic. In this case, the mean-square displacement is determined by both the elastic and the viscous response of the medium, and the dynamics of the particle depends strongly on the time scale at which it is probed. The elastic response of the medium is more important at short times, while the viscous response dominates at longer times. The effects of viscoelasticity are discussed in Sec. II A. A second complication of polymer solutions is that the continuum assumption is not valid on length scales smaller than the correlation length of the polymer network. For particles much larger than the correlation length the polymer solution behaves as a homogeneous fluid, but smaller particles see a discontinuous environment. The effects of the inhomogeneity of the medium are discussed in Sec. II B.

A. Effects of viscoelasticity of the medium

The Brownian motion of a particle of mass m in a viscoelastic medium can be described with a generalized Langevin equation [1]:

$$m \frac{dv(t)}{dt} = f_R(t) - \int_0^t \gamma(t-t')v(t')dt', \quad (4)$$

where $v(t)$ is the velocity of the particle, $f_R(t)$ denotes the random thermal forces on the particle causing the Brownian motion, and $\gamma(t)$ is a memory function. The integral term represents a force on the particle that depends on the velocity history rather than just on the momentary velocity as in the standard Langevin equation. Thus it reflects the viscoelasticity of the medium, with the possibility of storing energy in the medium and returning it to the particle at a later time. The exact form of $\gamma(t)$ depends on the relaxation mecha-

nisms playing a role in the medium. In the case of a Newtonian fluid with no memory it is given by a δ function: $\gamma(t) = \zeta_0 \delta(t)$. For this case, Eq. (4) reduces to the standard Langevin equation, and the mean-square displacement is given by Eqs. (1) and (2), if inertia is neglected.

Mason and Weitz [1] solved Eq. (4) for the general case in the Laplace domain. Furthermore, they related the memory function $\gamma(t)$ to the macroscopic shear modulus of the medium, by generalizing the Stokes-Einstein relation to all frequencies (see the Appendix). Thus, they obtained a direct relation between the mean-square displacement of the particle and the viscoelastic parameters of the medium. Van Zanten and Rufener considered the case where the forces on the particle can be described by a memory function with one single relaxation time [16]: $\gamma(t) = (\zeta/\tau)e^{-t/\tau}$, where $\zeta = \int_0^\infty \gamma(t)dt$ is the long-time friction coefficient and τ the relaxation time. It can be shown that this memory function corresponds to that of a particle moving in a continuous Maxwell fluid [16]. The Maxwell fluid is the simplest model for a viscoelastic material. Using this memory function, an analytical solution for $\langle \Delta r^2(t) \rangle$ can be obtained. Van Zanten and Rufener compared their predictions to experimental results for probe diffusion in wormlike micelle solutions. The macroscopic rheology of these solutions can be adequately described by the Maxwell model, at least in the frequency range accessible with mechanical rheometry [22,23]. Good agreement was found between the model and the experiments in the long-time behavior. At short times, however, they disagree. While the model predicts a ballistic regime [$\langle \Delta r^2(t) \rangle \sim t^2$] at short times due to the inertia of the particle, the experiments show a slower dynamics. The authors ascribed this to deviations from the Maxwell model at high frequencies due to Rouse and breathing modes.

Another factor which affects the short-time behavior of the probes is the friction of the background solvent, which is completely neglected by Van Zanten and Rufener [16]. This is justified as long as the viscous forces due to the solvent are much smaller than the viscoelastic forces due to the polymer matrix. At very short times the latter are small (the elastic force is proportional to the displacement), and the solvent viscosity cannot be neglected. In order to account for the background solvent, we split the memory function in a part coming from the polymer matrix and a part coming from the background solvent. The forces due to the polymer matrix are assumed to be Maxwellian and the solvent is Newtonian (this is equivalent to the Jeffreys model [26]). Figure 1 shows, schematically, the forces acting on the particle. The corresponding memory function is

$$\gamma(t) = \gamma_p(t) + \gamma_0(t) = \frac{\zeta_p}{\tau} e^{-t/\tau} + \zeta_0 \delta(t), \quad (5)$$

where ζ_p is the friction coefficient due to the polymer and ζ_0 that due to the solvent. Under certain conditions, the friction coefficients and the relaxation time τ can be connected to the macroscopic viscosity and elasticity, but we do not make this connection yet. In this section we only consider the local

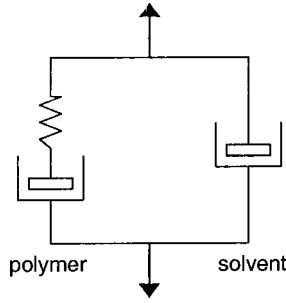


FIG. 1. A schematic representation of the forces acting on a particle in a polymer solution. The friction forces due to the solvent are represented by a Newtonian dashpot, and the friction and elastic forces due to the polymer matrix by a dashpot and an elastic spring connected in series.

friction and elastic forces that a particle experiences. The relation with the macroscopic viscosity and elasticity will be discussed in Sec. II B.

If inertia is neglected (which is justified for $t \gg m/\zeta_0$), Eq. (4) with Eq. (5) can be solved exactly (see the Appendix):

$$\langle \Delta r^2(t) \rangle = \frac{6kT}{\zeta} \left[t + \tau \left(1 - \frac{\zeta_0}{\zeta} \right) \left\{ 1 - \exp\left(-\frac{\zeta t}{\zeta_0 \tau} \right) \right\} \right], \quad (6)$$

where $\zeta = \zeta_p + \zeta_0$. This reduces to the result of Van Zanten and Rufener [16] for $\zeta_0 = 0$. The term ζ_0/ζ may be neglected if the long-time friction due to the polymer solution is much larger than the short-time friction due to the solvent alone. Doing this, we can rewrite Eq. (6) as

$$\langle \Delta r^2(t) \rangle = 6\delta^2 \left[1 - \exp\left(-\frac{D_s t}{\delta^2} \right) \right] + 6D_l t, \quad (7)$$

where $D_s = kT/\zeta_0$ and $D_l = kT/\zeta$ are the short-time and long-time diffusion coefficients, respectively, and where $\delta^2 = kT\tau/\zeta$. We will now discuss the limiting behaviors of Eq. (7).

At short times ($t \ll \delta^2/D_s$), the viscous force due to the solvent $\zeta_0 v(t)$ dominates over the elastic force due to the polymer matrix, which is proportional to the particle displacement. Thus the motion is diffusive at these time scales: $\langle \Delta r^2(t) \rangle = 6D_s t$. At longer times the particle slows down as a result of the elastic forces exerted by the polymer matrix, and $\langle \Delta r^2(t) \rangle$ finally saturates at a plateau value $6\delta^2$. At these time scales the particle moves about within an elastic cage formed by the polymers. The magnitude of the plateau displacement is determined by the elasticity of the polymer network. In Sec. II B, we will relate it to the macroscopic elastic modulus. At even longer times the elastic cages themselves fluctuate due to the reptation (and in the case of living polymers also the breaking) of polymer chains. The polymers forming the cage are completely relaxed at $t > \tau$. The viscoelastic response is dominated by the viscous component at these time scales, and the motion is again diffusive:

$$\langle \Delta r^2(t) \rangle = 6(\delta^2 + D_l t), \quad (8)$$

which is exactly the inertialess result of Van Zanten and Rufener, who neglected the solvent [16].

The first term on the right-hand side of Eq. (7) describing the short-time dynamics is exactly the same as that found for a Brownian particle in a harmonic potential, $U(r) = \frac{1}{2}Kr^2$ where K is an elastic constant [13,27]. The maximum displacement in this potential can be found by equating the potential energy and the thermal energy of the particle ($\frac{3}{2}kT$). This gives $r_{max} = 6\delta^2 = 3kT/K$. Comparing this to Eq. (7), we see that the effective spring constant felt by the particles is $K = \zeta/2\tau$. The harmonically bound particle model was used by several authors to describe the particle motion in concentrated colloidal suspensions and colloidal glasses [13]. It has also been used to describe Brownian motion in gels [7]. Bellour *et al.* [18] suggested that the liquid state of the polymer solution at long times can be accounted for by multiplying the mean-square displacement of the harmonically bound particle with a factor $(1 + D_l t/\delta^2)$. Thus they arrived at an expression which is very similar to our Eq. (7), although not exactly the same. A similar approach was followed by Fadda *et al.* [9]. Here we have given a more rigorous justification of Eq. (7).

B. Relation to the macroscopic rheology and effects of inhomogeneity of the medium

In this section, we discuss the connection between the friction and elastic forces experienced by the particle and the macroscopic viscosity and elasticity of the polymer solution. At short times, the friction forces due to the solvent dominate and the friction experienced at these times is given by the solvent viscosity: $\zeta_0 = 6\pi\eta_0 R$. (Hydrodynamic interactions between the particles and the polymer chains may reduce the short-time diffusion coefficient somewhat, but here we neglect this.) At longer times the forces exerted by the polymers are more important. Above the overlap concentration c^* , the polymers are entangled and form a continuous network, characterized by a correlation length ξ (the mesh size of the network). When the particles are much larger than the correlation length (i.e., $R \gg \xi$), the medium can be considered as a continuum for the particles. It is expected that the particles experience the macroscopic properties of the medium in this case. The friction force experienced by the particles is then given by the Stokes-Einstein relation [Eq. (3)] with η the macroscopic viscosity, and the relaxation time τ in the memory function is equal to the macroscopic relaxation time of the medium [16], which can be measured with mechanical rheometry. This gives the following relation between the plateau displacement and the elasticity of the medium:

$$\delta^2 = \frac{kT\tau}{\zeta} = \frac{kT}{6\pi R G_0}, \quad (9)$$

where $G_0 = \eta/\tau$ is the elastic plateau modulus. A more general relation between the mean-square displacement and the viscoelastic parameters of the medium (in the Laplace domain) was derived by Mason and Weitz [1] (see the Appendix).

Probe particles that are smaller than the correlation length ($R < \xi$) see a discontinuous environment. These particles are not trapped in the polymer network, but they can slip through the meshes of the network. Hence, the friction experienced by these probes is much smaller than expected on the basis of the macroscopic viscosity η . Very small particles ($R \ll \xi$) move through the network without noticing the polymer, and feel only the solvent viscosity η_0 . Intermediate particles feel an effective friction which lies between η_0 and η . A scaling model for the motion of small particles through a statistical network was developed by Langevin and Rondelez [28]. They considered diffusion as an activated process, with an activation energy which is determined by the elastic distortion of the network due to the moving particle. They arrived at the following result:

$$\frac{D_I}{D_0} = \exp[-(R/\xi)^\alpha], \quad (10)$$

where D_I and D_0 are the diffusion coefficients in the polymer solution and in pure solvent, respectively, and α is a scaling exponent. Since the correlation length decreases with concentration as $\xi \sim c^{-\nu}$, the diffusion coefficient decreases as a stretched exponential with concentration, $D_I/D_0 \sim \exp[-aR^\alpha c^\beta]$. Other authors have used different assumptions, but found similar expressions [2,29,30]. Equation (10) seems to adequately describe the measured diffusion coefficients of probe particles as long as R is smaller than ξ , but for larger particles ($R \gtrsim \xi$) deviations are often found [31,32]. This can be explained by the fact that in the derivation of Eq. (10), the fluctuations in the polymer network due to the reptation of the polymer chains are neglected. In the regime where $R \gtrsim \xi$, both the activated diffusion through the meshes of the network and the mobility of the polymer chains play a role. Hence, the diffusion coefficient becomes a function of both the viscosity η and the ratio R/ξ . There are at present no theories that give a satisfactory description of this regime.

III. EXPERIMENT

Self-associating monomers. The synthesis and characterization of the self-associating monomers [bis(ethylhexylureido)toluene, or EHUT] were described elsewhere [24,25]. These monomers have been shown to form long polymer chains in various solvents, as a result of reversible hydrogen bonding between the monomers (see Fig. 2). Samples were prepared by dissolving EHUT in cyclohexane (analytical grade) at room temperature, under stirring for at least one night.

Probe particles. Silica particles modified with a hydrophobic alkyl layer were used as probe particles. Monodisperse silica particles (Merck monospher) with radii of 125 and 250 nm were coated with a hydrophobic octadecanol layer using the method described by Van Helden *et al.* [33]. Particles were added to the polymer samples from a concentrated stock suspension in cyclohexane.

Rheology of EHUT solutions. The viscosities of the low-concentration EHUT solutions were measured with a PVS1 Lauda capillary viscosimeter. A Paar Physica MCR 300 rhe-

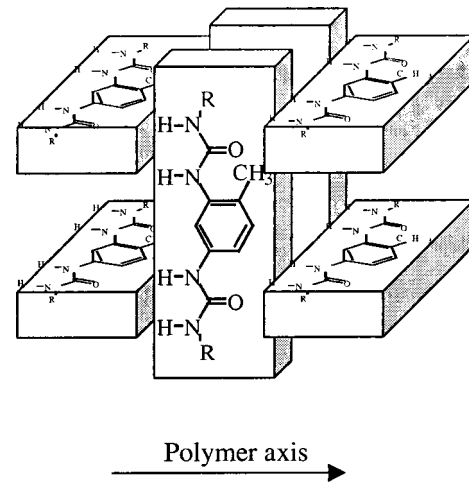


FIG. 2. A schematic representation proposed for the reversible polymerization of the EHUT monomers. (Taken from Lortie *et al* [25].)

ometer, equipped with a 50-mm cone and plate geometry, was used to determine the zero-shear viscosity at higher concentrations. At intermediate concentrations the capillary viscosimeter and the rheometer give the same values for the viscosity. Dynamic shear measurements were performed in an angular frequency range between $\omega = 0.05$ and $\omega = 80 \text{ rad s}^{-1}$. The temperature was kept at 25.0°C using a Peltier element. A solvent trap was used to minimize evaporation during the measurement. It was checked that adding probe particles to the EHUT solutions did not change the rheology.

Static light scattering by EHUT solutions. Light scattering experiments were performed using an Argon laser (wavelength $\lambda = 514.5 \text{ nm}$) at various scattering angles θ between 25 and 140° , corresponding to scattering vectors $q = (4\pi n/\lambda)\sin(\theta/2)$, where $n = 1.4262$ is the refractive index of the solvent (cyclohexane), between 7.5×10^{-3} and $3.3 \cdot 10^{-2} \text{ nm}^{-1}$. Static measurements were done with toluene as a reference (Rayleigh ratio equal to $2.9 \times 10^{-3} \text{ m}^{-1}$), in a concentration range between 0.4 and 8 g/l (in the semidilute regime). The correlation length ξ of the polymer network can be obtained using the Ornstein-Zernike relation for the structure factor [34]:

$$I(q) \sim \frac{1}{1 + q^2 \xi^2}. \quad (11)$$

Plots of $1/I(q)$ versus q^2 are indeed straight lines, and ξ can be obtained from the ratio between the slope and the intercept.

Dynamic light scattering by probe particles. Dynamic light scattering measurements were done with the same setup as described above, using an ALV5000 digital correlator to calculate the intensity correlation function. The concentration of the probe particles was adjusted such that the scattered intensity of the probe particles was at least 20 times that of the polymer solution without the particles. The contribution of the scattering of the polymer matrix to the cor-

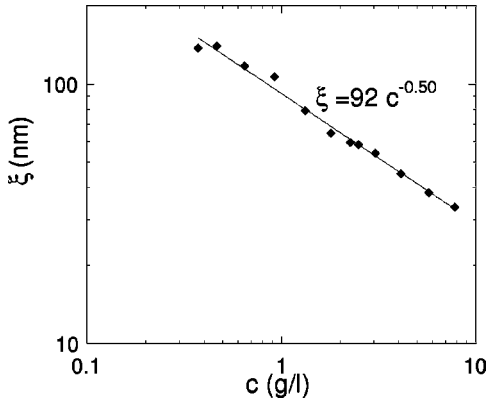


FIG. 3. The correlation length of EHUT in cyclohexane at 25.0 °C as a function of the concentration.

relation function was then neglected. In all cases the particles were dilute with a volume fraction $\phi = 0.0005$ for the 250 nm particles and $\phi = 0.002$ for the 125-nm particles, so that particle-particle interactions are negligible. The temperature was 25.0 °C.

The intensity correlation function is defined as $g^{(2)}(t) = \langle I(\tau)I(\tau+t) \rangle / \langle I(\tau) \rangle^2$. The experimental correlation function is related to the normalized field autocorrelation function $g^{(1)}(t)$:

$$g^{(2)}(t) = 1 + A[g^{(1)}(t)]^2, \quad (12)$$

where A is a constant that depends on the experimental setup. Assuming Gaussian statistics, the mean-square displacement of the particles can be calculated from $g^{(1)}(t)$ [13]:

$$g^{(1)}(t) = \exp\left[-\frac{q^2}{6}\langle \Delta r^2(t) \rangle\right]. \quad (13)$$

Measurements performed at various scattering angles showed that, within experimental noise, the quantity $q^{-2} \ln[g^{(1)}(t)]$ is independent of the scattering vector. Hence, non-Gaussian contributions to the particle displacement, which would result in deviations from Eq. (13) at long times [15], are rather small. Most measurements presented here were done at 90° ($q = 2.5 \times 10^{-2} \text{ nm}^{-1}$).

IV. RESULTS AND DISCUSSION

A. Polymer solutions without probes

Figure 3 shows the correlation length ξ , measured with static light scattering, as a function of the concentration c . The data are very well fitted by a power law $\xi = 92c^{-0.5}$. This scaling is expected for isotropic semidilute rigid rods or for semiflexible chains if the persistence length l_p is larger than the correlation length ξ [29]. We may therefore conclude that the persistence length of the polymers is at least 100 nm. Small-angle neutron scattering data for the same molecules in toluene have indeed shown that the scattering data could be described by a form factor for rigid rods [25]. So far, we have not been able to measure the persistence length precisely.

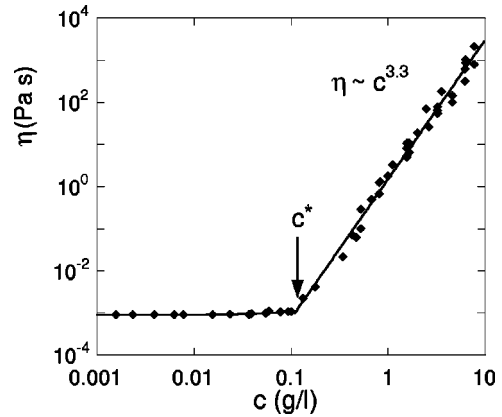


FIG. 4. The viscosity of EHUT in cyclohexane at 25.0 °C as a function of the concentration.

The viscosity of the supramolecular polymer solutions as a function of the concentration c is shown in Fig. 4. Clearly, two regimes are visible. The crossover between these two regimes occurs at a concentration $c^* \approx 0.11 \text{ g/l}$ ($= 0.25 \text{ mM}$). Below c^* , the viscosity increases only little with concentration. Above c^* the viscosity increases very rapidly, and can be fitted with a power law: $\eta = 1.5c^{3.3}$. This strong increase of the viscosity is a result of the formation of polymer chains. With increasing concentration, the chains grow longer [22,23], and at high concentrations they form a strongly entangled network with high viscosity. The crossover concentration c^* is generally identified with the onset of entanglements. While for regular polymers this may be significantly above the overlap concentration, living polymers are likely to entangle as soon as they overlap, because of the rapid growth of the chains around c^* [35]. Therefore we may assume that c^* corresponds to the overlap concentration.

Figure 5 shows the storage modulus G' (the elastic component) and the loss modulus G'' (the viscous component) as a function of the angular frequency ω for two polymer concentrations. The results show the viscoelastic nature of the polymer solutions. At low frequencies, the mechanical response is dominated by the loss modulus. At higher frequen-

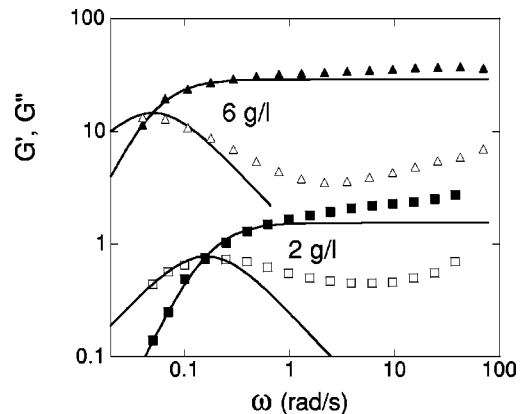


FIG. 5. The storage modulus G' (■, ▲) and the loss modulus G'' (□, △) as a function of the angular frequency ω for two concentrations. The full curves are fits to the Maxwell model.

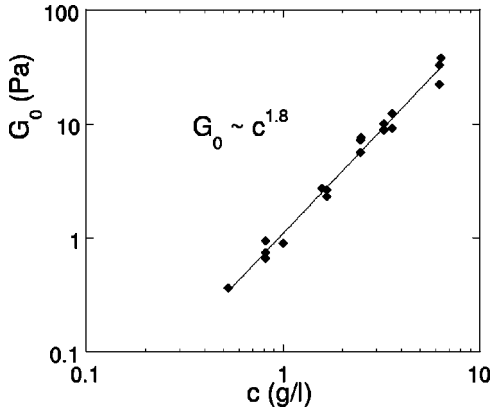


FIG. 6. Elastic plateau modulus G_0 of EHUT in cyclohexane at 25.0 °C as a function of the concentration. The full line is a fit to a power law.

cies the storage modulus is predominant and reaches a plateau value, while the loss modulus passes a maximum and then a minimum. At low frequencies, the data can be fitted reasonably well with the single relaxation time Maxwell model (the full curves in Fig. 5), but at high frequencies deviations from this model occur. The high frequency plateau of the storage modulus G_0 , as obtained from the fit to the Maxwell model, is plotted in Fig. 6 as a function of the concentration c . The results can be fitted with a power law $G_0 = 1.2c^{1.8}$.

We may compare our rheological results to theoretical predictions. Cates [23] proposed a model for the stress relaxation in living polymer solutions, based on the reptation theory of Doi and Edwards [27]. He showed that the stress relaxation at low frequencies is governed by a single relaxation time (Maxwell behavior), provided that the breaking of the chains is fast compared to the reptation time. At higher frequencies other relaxation mechanisms play a role and deviations from Maxwell behavior occur. This is in agreement with our results of Fig. 5. If the polymer chains would be rigid rods, the plateau modulus G_0 would be proportional to the number concentration of rods, and independent of the rod length [27]. For living polymers this would give G_0

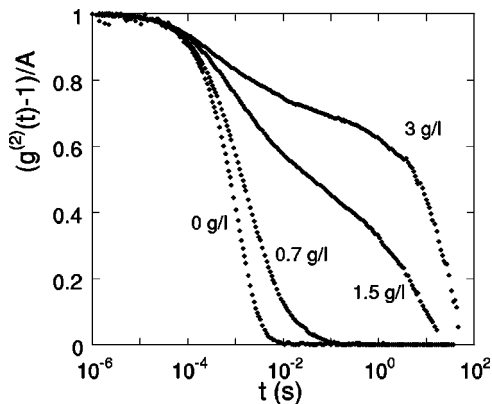


FIG. 7. Normalized intensity correlation functions measured at $\theta = 90^\circ$ for probes of 250-nm radius in EHUT solutions of varying concentration at 25.0 °C.

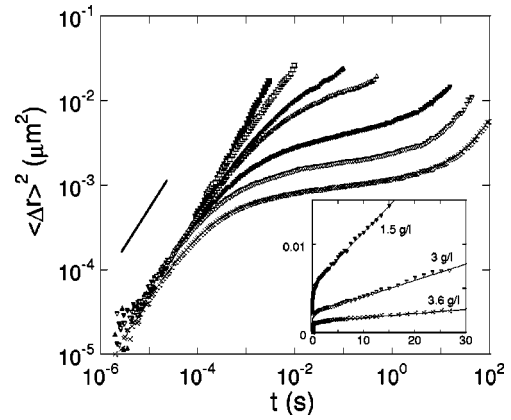


FIG. 8. Mean-square displacement of 250-nm probes in pure cyclohexane (■), and in EHUT solutions of 0.14 (□), 0.67 (▲), 0.79 (△), 1.5 (▼), 3.0 (▽), and 3.6 (×) g/l. Large figure: on a logarithmic scale; the line with slope 1 indicates diffusive motion. Inset: on a linear scale; full lines are fits to Eq. (8).

$\sim c/\langle L \rangle \sim c^{1/2}$ [36], which is lower than we find here. For flexible chains, on the other hand, $G_0 \sim c^{9/4}$ is predicted for both regular and living polymers [23,27,36], which is higher than we observe. From the measured correlation lengths (Fig. 3) we expect that the EHUT polymers are semiflexible with a persistence length larger than the correlation length. For semiflexible chains an exponent 7/5 was proposed [37] and found experimentally for actin filaments [38]. This is somewhat smaller than we find here. Perhaps our supramolecular polymers have a smaller persistence length than actin, and therefore the exponent is closer to the flexible chain scaling. The scaling of the viscosity with concentration is in reasonable agreement with the model of Cates. The exponent of 3.3 lies between the scaling expected for flexible chains and rigid rods [23,36]. It is also comparable to experimental values found for several wormlike micelle systems [22].

B. Probe diffusion

Figure 7 shows typical correlation functions measured with dynamic light scattering for probes of 250-nm radius in polymer solutions of different concentrations. In pure solvent the correlation function is a simple exponential decay. With increasing polymer concentration the curves shift toward longer times, indicating that the particles are slowed down by the polymer. Furthermore, the decay is no longer a simple exponential at high polymer concentrations, but it appears to be double exponential.

Figure 8 shows the mean-square displacement $\langle \Delta r^2(t) \rangle$ of the particles calculated from the correlation function using Eq. (13). The evolution of the particle motion with concentration is clearly observed in this figure. In pure solvent and at very low polymer concentrations, $\langle \Delta r^2(t) \rangle$ is proportional to time, indicating diffusive motion of the particles, as given by Eq. (1). The measured diffusion coefficient D_0 is in agreement with the Stokes-Einstein Eqs. (2) and (3). When the concentration is of the order of c^* or larger, deviations from Eq. (1) are observed. The particle motion is now no longer simple diffusion. Three regions can be observed in Fig. 8. At short times the motion is diffusive (slope equal to 1) with a short-time diffusion coefficient which is, within the

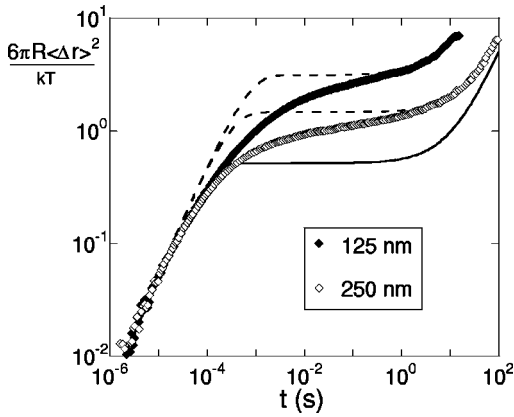


FIG. 9. Comparison between experimentally determined $\langle \Delta r^2(t) \rangle$ and Eq. (7) for two particle sizes at a polymer concentration of 3.6 g/l. Dashed curves are fits to Eq. (7); the full curve corresponds to the macroscopic viscoelastic parameters.

experimental accuracy, independent of the polymer concentration equal to that in pure cyclohexane: $D_s \approx D_0$. At intermediate time scales there is a transition region where the particles are slowed down. At very long times finally, the motion is diffusive again, but with a diffusion coefficient D_l which is much smaller than D_0 . The long-time diffusion is more clearly seen when $\langle \Delta r^2(t) \rangle$ is plotted on a linear scale (see the inset in Fig. 8). Equation (8) adequately describes the data in this region. Both the short-time and the long-time dynamics of the probe particles are in qualitative agreement with Eq. (7). A more quantitative comparison between the experimental data and the theoretical prediction of Eq. 7 is shown in Fig. 9 for the two particle sizes at a polymer concentration of 3.6 g/l. The correlation length at this concentration is 48 nm. Since both particles are larger than the correlation length, we would expect the particles to be trapped in the polymer network, and to experience the macroscopic viscoelastic properties. According to Eqs. (7), (3), and (9), rescaling of the data as $6\pi R \langle \Delta r^2(t) \rangle / kT$ should result in one single curve for both particle sizes. In fact, it has been shown by Xu *et al.* that this should be equal to the macroscopic creep compliance of the medium [11]. Clearly, the data do not collapse onto one curve. Fits of the data to Eq. (7) are plotted in Fig. 9 as well. The parameters in this equation are obtained from fits in the appropriate region: D_s from the initial linear part of the curve, and D_l and δ^2 from a fit in the long-time linear region to Eq. (8) (see inset in Fig. 8). In the same figure, we have plotted the prediction of Eq. (7) with values of the parameters as given by Eqs. (3) and (9) and the measured macroscopic viscosity and elastic modulus. It is clear that the experimental values of δ^2 and D_l are larger than expected on the basis of the macroscopic viscoelastic properties. Also the shape of the measured mean-square displacement is different than predicted by Eq. (7): the experimental data do not show a true plateau, but a more smooth transition region.

In the derivation of Eq. (7) we have assumed that the polymer network can be described as a Maxwell model with one relaxation time τ . At $t < \tau$ there is no stress relaxation, and the polymer network behaves as an elastic spring for the

particle. This causes the plateau in $\langle \Delta r^2(t) \rangle$. Most polymer solutions, however, cannot be described by the Maxwell model at very short times (or high frequencies). Other relaxation mechanisms than reptation play a role at short times, which cause fluctuations of the elastic cages on these time scales. As a result, $\langle \Delta r^2(t) \rangle$ does not reach a true plateau, but there is a smooth transition region. Indeed, we see in Fig. 5 that the Maxwell model does not describe the data at high frequencies. In Fig. 9 we see that the differences between the experimental data and Eq. (7) are largest at the onset of the transition region. Unfortunately, the frequencies corresponding to this region are inaccessible with mechanical rheometry. Hence, it is not possible to make a direct comparison between the microscopic information obtained from $\langle \Delta r^2(t) \rangle$ and the macroscopic shear moduli G' and G'' in this region. A model for the viscoelastic properties of entangled semiflexible polymers was developed by Morse [39]. This model predicts that, after the plateau region in G' at intermediate frequencies, the dynamic shear moduli increase as $G'(\omega) \approx G''(\omega) \sim \omega^{3/4}$ at very high frequencies (far beyond the range of Fig. 5). According to the model of Mason and Weitz [1,11], this scaling would result in subdiffusive behavior at short times with $\langle \Delta r^2(t) \rangle \sim t^{3/4}$. This was indeed observed for probe particles in solutions of actin filaments [11]. We do not observe such a scaling in our results over a significant time scale, however. The reason for this is not clear. Perhaps the stress due to the solvent dominates the high frequency response of the polymer matrix for the present case. Alternatively, the possibility of the supramolecular chains to break and recombine may result in different relaxation mechanisms at high frequencies than for unbreakable polymers, and, hence, in a different dynamics of the particles at short times.

Even though the Maxwell model fails at short times, it should still provide a good description at long times (i.e., low frequencies). The values found for D_l and δ^2 from a fit to Eq. (8) at long times should then correspond to the viscosity and the longest relaxation time of the medium.

In Fig. 10 the measured short-time and long-time diffusion coefficients are plotted as a function of the polymer concentration for both particle sizes. As already mentioned, the short-time diffusion coefficient is independent of the polymer concentration and equal to the diffusion coefficient in pure cyclohexane. This shows that hydrodynamic interactions between the particles and the polymer chains at short times are unimportant. The long-time diffusion coefficient D_l , on the other hand, decreases by orders of magnitude as the polymer concentration increases. The full line with slope -3.3 gives the prediction according to the Stokes-Einstein relation (3), using the viscosity data of Fig. 4. At the highest concentrations, the measured D_l seem to be in reasonable agreement with the Stokes-Einstein values. At lower concentrations, however, the particles experience a smaller friction than expected on the basis of the macroscopic viscosity. For smaller particles the deviations are larger. The deviations from the Stokes-Einstein relation can be ascribed to small-particle effects. The correlation length (Fig. 3) varies between 135 and 30 nm going from 0.47 to 7.3 g/l. Hence, R/ξ varies between 0.9 and 4.2 for the 125-nm particles and be-

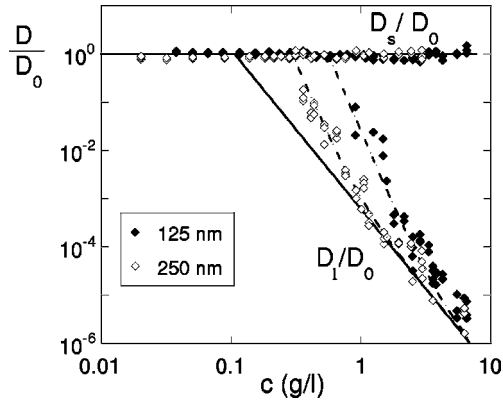


FIG. 10. Short-time and long-time diffusion coefficients of probes in EHUT solutions relative to the diffusion coefficient D_0 in cyclohexane. Filled symbols, $R=125$ nm; open symbols, $R=250$ nm. The horizontal full line indicates the Stokes-Einstein relation in the solvent ($D_s=D_0$), and the one with slope -3.3 that according to the macroscopic viscosity ($D_l/D_0=\eta_0/\eta$).

tween 1.9 and 8.3 for the 250-nm particles. At low polymer concentrations, R and ξ are of the same order of magnitude, and the continuum assumption is not valid, especially for the smallest particles.

We expect that the diffusion coefficient is a function of R/ξ . We tried fitting our data to the model of Langevin and Rondelez [28], Eq. (10), but found no good agreement. The reason for this is probably that this model neglects the effect of the mobility of the polymer chains. We found that our data can be fitted with the following equation (see the dashed curves in Fig. 10):

$$\frac{D}{D_0} = \frac{\eta_0}{\eta} \left[1 + 600 \left(\frac{\xi}{R} \right)^6 \right]. \quad (14)$$

The factor η_0/η accounts for the relaxation of the polymer chains forming the cages of the particles, while the factor in brackets reflects the extra mobility due to the moving of particles through the network meshes. For $\xi/R \rightarrow 0$ the latter is negligible, and Eq. (14) reduces to the Stokes-Einstein relation (3) (see the drawn line with slope -3.3 in Fig. 10). Equation (14) is empirical; so far, we do not have a physical justification.

An alternative explanation for a friction lower than given by Eq. (3) was given by Donath *et al.* [40]. They calculated the friction factor for a particle surrounded by a depletion zone. It is well known that colloidal particles in a nonadsorbing polymer solution are surrounded by a polymer-poor depletion zone as a result of the entropy loss that chains suffer near the particle surface [41]. Donath *et al.* predicted that the presence of such a depletion layer results in a friction that is lower than $6\pi\eta R$ by at most a factor $2/3$ [40]. The deviations from Eq. (3) observed in our experiments are much larger than this, however. Hence, the depletion effect cannot explain our results.

Figure 11 shows $6\pi R\delta^2/kT$, with δ obtained from a fit of the experimental data to Eq. (8) (e.g., inset Fig. 8), as a function of the concentration for both particle sizes. Accord-

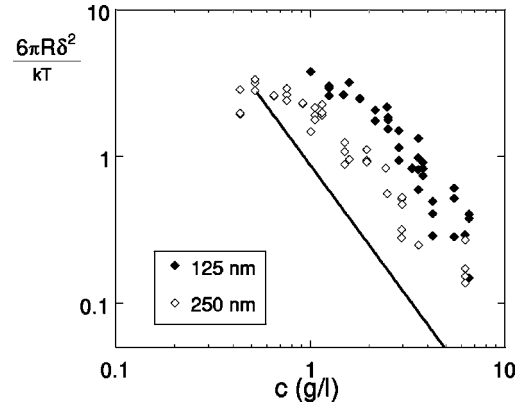


FIG. 11. Normalized plateau displacement $6\pi R\delta^2/kT$ as a function of EHUT concentration for both particle sizes. The full line with slope -1.8 corresponds to Eq. (9) with the macroscopic plateau modulus shown in Fig. 6.

ing to the microrheology model, Eq. (9), this should correspond to the reciprocal plateau modulus $1/G_0=\tau/\eta$. The macroscopic data are plotted in this figure, too. It is clear that the values of δ^2 are systematically higher than expected on the basis of the macroscopic elastic moduli at high concentrations, while at lower concentrations they seem to intersect. The difference between the measured values of δ^2 and the predictions according to Eq. (9) is larger for smaller particles, but in contrast to what we observed for the diffusion coefficients D_l , the differences do not become smaller with increasing concentration. Hence, it seems that the difference is not only caused by the ratio R/ξ , but also by other factors. At high concentrations, δ^2 is larger than expected on the basis of the elastic modulus. Hence, the distance that the particles can travel before they are pushed back by the elastic forces of their microscopic cage is larger than expected. A reason for this may be the presence of a depletion layer around the particles with low viscosity [42]. This depletion layer could be regarded as an effective increase of the size of the microscopic cage of the particles, and would thus result in a larger δ^2 . Another factor which may play a role is the semiflexibility of the chains. A semidilute solution of flexible chains is fully described by one length scale, the correlation length ξ . For semiflexible chains, however, there is a second principal length scale, the persistence length l_p (and for rods the total length L). Therefore, the condition $R \gg \xi$ may not be sufficient to ensure that the particle feels the macroscopic properties, but also $R \gg l_p$ (or for rods $R \gg L$) may be required [37]. Indeed, experiments for actin filaments of different length have shown that this second condition is necessary [12]. For supramolecular polymers, the average length L increases with increasing concentration, and thus R/L decreases. This would explain that even at high polymer concentrations there is still a large difference between the measured δ^2 and Eq. (9). Only when R is larger than both L and ξ we may expect agreement.

In the interpretation of the dynamic light scattering results, we have assumed that the only contribution to the measured intensity correlation function is the self-correlation function of the particles. The scattering of the polymer

chains is completely neglected. However, the particle-polymer partial dynamic structure factor describing the correlations between the position of a particle and the positions of the surrounding polymer chains may not be completely negligible. Its amplitude is $(I_1 I_2)^{1/2}$ with I_1 and I_2 the scattered intensities of particles and polymer, respectively. At the highest polymer concentrations (where $I_1 \approx 20I_2$), this is only about 4.5 times smaller than the amplitude of the self-correlation function of the particles (I_1). Neglecting the particle-polymer cross term for these concentrations is not really justified, and some of the disagreement between experiment and theory may therefore be caused by this effect.

V. CONCLUDING REMARKS

We have used dynamic light scattering to measure the Brownian motion of colloidal particles in a solution of hydrogen-bonded supramolecular polymers. At short times the motion is governed by the viscosity of the solvent, while at longer times it is determined by the viscoelastic properties of the polymer matrix. An equation was derived for the mean-square displacement of a particle in a viscoelastic medium consisting of a Maxwell-like polymer matrix and a Newtonian background solvent. This model predicts the short-time diffusive behavior correctly. At intermediate and long times, it agrees qualitatively with the experiments, but there are significant differences between the two. The long-time diffusion is faster than expected on the basis of the macroscopic viscosity if the size of the probes is not sufficiently larger than the correlation length of the polymer network. Furthermore, the ‘‘plateau’’ mean-square displacement is larger than would be expected on the basis of the macroscopic elastic modulus. Some of these differences can be explained by the possibility of the particles to move through the meshes of the network if R/ξ is not large enough. Other possible reasons for the differences are a depletion zone around the particles with lower viscosity than in the bulk and the effect of the stiffness of the chains. Clearly, a satisfactory theoretical description of the Brownian motion in polymer solutions, which takes into account all these effects, is lacking.

APPENDIX

In this appendix we show how the generalized Langevin equation can be solved for the memory function given by Eq. (5), and how $\langle \Delta r^2(t) \rangle$ is related to the dynamic shear modulus. The random force $f_R(t)$, which drives the Brownian motion, is assumed to be a Gaussian variable with zero mean. It is not correlated to the previous values of the particle velocity: $\langle v(0)f_R(t) \rangle = 0$. The average velocity is set by the equipartition theorem of thermal energy: $m \langle v(t)v(t) \rangle = 3kT$. Using this, the generalized Langevin equation (4) can be solved by taking the Laplace transform $\tilde{g}(s) \equiv \int_0^\infty e^{-st} g(t) dt$. Multiplication by the initial velocity $v(0)$ and ensemble averaging then gives the velocity corre-

lation function $\langle v(0)\tilde{v}(s) \rangle$. From this, we can obtain a relation between the mean-square displacement and the memory function in the Laplace domain [1]:

$$\langle \Delta r^2(s) \rangle = \frac{6kT}{s^2[\tilde{\gamma}(s) + ms]}. \quad (\text{A1})$$

The inertial term ms can be neglected, except at very short times. Inserting the Laplace transform of the memory function (5) we find (neglecting inertia)

$$\langle \Delta r^2(s) \rangle = \frac{6kT(1 + \tau s)}{s^2[\zeta_p + \zeta_0(1 + \tau s)]}. \quad (\text{A2})$$

Laplace inversion then gives the mean-square displacement in the time domain, Eq. (6).

Mason and Weitz tried to connect the mean-square displacement directly to the dynamic shear modulus of the medium. They assumed that the Stokes-Einstein relation is valid at all frequencies [1]:

$$\tilde{\gamma}(s) = 6\pi R \tilde{\eta}(s) = 6\pi R \frac{\tilde{G}(s)}{s}, \quad (\text{A3})$$

where $\tilde{\eta}(s)$ is the frequency-dependent viscosity, and $\tilde{G}(s)$ is the Laplace transformed shear modulus. This equation is exact for a viscous fluid with no-slip boundary conditions, but it is approximate for viscoelastic liquids. Equation (A1) with Eq. (A3) gives a direct relation between the Brownian motion of the particle and the viscoelastic parameters of the medium. It has been used by several authors to measure the viscoelastic parameters of complex fluids at high frequencies.

The linear viscoelastic properties of materials are usually measured using oscillatory shear measurements, and characterized by the complex shear modulus $G^*(\omega) = G'(\omega) + iG''(\omega)$, where G' and G'' are the storage and loss moduli. This complex modulus gives the response of the fluid to a macroscopic oscillatory deformation with frequency ω . It can be obtained from $\tilde{G}(s)$ using analytical continuation, substituting $i\omega$ for s , and taking the real and imaginary parts for G' and G'' , respectively [1]. Using the memory function (5), we find

$$G'(\omega) = \frac{\eta_p \omega^2 \tau}{1 + \omega^2 \tau}, \quad (\text{A4})$$

$$G''(\omega) = \frac{\eta_p \omega}{1 + \omega^2 \tau} + \eta_0 \omega, \quad (\text{A5})$$

i.e., the viscoelastic moduli of a single relaxation time Maxwell fluid plus a Newtonian contribution of the solvent. This is the solution of the constitutive equation for a Jeffreys model [26] (see Fig. 1).

- [1] T.G. Mason and D.A. Weitz, *Phys. Rev. Lett.* **74**, 1250 (1995).
- [2] G.D.J. Phillies, G.S. Ullmann, K. Ullaman, and T. Lin, *J. Chem. Phys.* **82**, 5242 (1985).
- [3] K.L. Ngai, G.D.J. Phillies, and T. Lin, *J. Chem. Phys.* **105**, 8385 (1996).
- [4] D.E. Dunstan and J. Stokes, *Macromolecules* **33**, 193 (2000).
- [5] J. Won, C. Onyenemezu, W. Miller, and T.P. Lodge, *Macromolecules* **27**, 7389 (1994).
- [6] X.Y. Ye, P. Tong, and L.J. Fetters, *Macromolecules* **31**, 5785 (1998).
- [7] G. Nisato, P. Hébraud, J.-P. Munch, and S.J. Candau, *Phys. Rev. E* **61**, 2879 (2000).
- [8] T. Narita, A. Knaebel, J.-P. Munch, and S.J. Candau, *Macromolecules* **34**, 8224 (2001).
- [9] G.C. Fadda, D. Lairez, and J. Pelta, *Phys. Rev. E* **63**, 061405 (2001).
- [10] M. Shibayama, Y. Isaka, and Y. Shiwa, *Macromolecules* **32**, 7086 (1999).
- [11] J. Xu, V. Viasnoff, and D. Wirtz, *Rheol. Acta* **37**, 387 (1998).
- [12] F.G. Schmidt, B. Hinner, and E. Sackmann, *Phys. Rev. E* **61**, 5646 (2000).
- [13] P.N. Pusey and R.J.A. Tough, in *Dynamic Light Scattering*, edited by R. Pecora (Plenum Press, New York, 1985), p. 85.
- [14] S.G.J.M. Kluijtmans, G.H. Koenderink, and A.P. Philipse, *Phys. Rev. E* **61**, 626 (2000).
- [15] W. Van Megen, T.C. Mortensen, S.R. Williams, and J. Müller, *Phys. Rev. E* **58**, 6073 (1998).
- [16] J.H. Van Zanten and K.P. Rufener, *Phys. Rev. E* **62**, 5389 (2000).
- [17] P.A. Hassan and C. Manohar, *J. Phys. Chem. B* **102**, 7120 (1998).
- [18] M. Bellour, M. Skouri, J.-P. Munch, and P. Hébraud, *Eur. Phys. J. E* **8**, 431 (2002).
- [19] J.-M. Lehn, *Supramolecular Chemistry, Concepts and Perspectives* (VCH, Weinheim, 1995).
- [20] A. Ciferri, *Supramolecular Polymers* (Marcel Dekker, New York, 2000).
- [21] L. Brunsveld, B.J.B. Folmer, E.W. Meijer, and R.P. Sijbesma, *Chem. Rev. (Washington, D.C.)* **101**, 4071 (2001).
- [22] M.E. Cates and S.J. Candau, *J. Phys.: Condens. Matter* **2**, 6869 (1990).
- [23] M.E. Cates, *Macromolecules* **20**, 2289 (1987).
- [24] S. Boileau, L. Bouteiller, F. Lauprêtre, and F. Lortie, *New J. Chem.* **24**, 845 (2000).
- [25] S. Lortie, F. ad Boileau, L. Bouteiller, C. Chassenieux, B. Demé, G. Ducouret, M. Jalabert, F. Lauprêtre, and P. Terech, *Langmuir* **18**, 7218 (2002).
- [26] H.A. Barnes, J.F. Hutton, and K. Walters, *An Introduction to Rheology* (Elsevier, Amsterdam, 1989).
- [27] M. Doi and S.F. Edwards, *The Theory of Polymer Dynamics* (Clarendon Press, Oxford, 1986).
- [28] D. Langevin and F. Rondelez, *Polymer* **19**, 875 (1978).
- [29] A.G. Ogston, B.N. Preston, and J.D. Wells, *Proc. R. Soc. London, Ser. A* **333**, 297 (1973).
- [30] R.I. Cukier, *Macromolecules* **17**, 252 (1984).
- [31] S.P. Radko and A. Chrumbach, *Macromolecules* **32**, 2617 (1999).
- [32] P. Tong, X. Ye, B.J. Ackerson, and L.J. Fetters, *Phys. Rev. Lett.* **79**, 2363 (1997).
- [33] A.K. Van Helden, J.W. Jansen, and A. Vrij, *J. Colloid Interface Sci.* **81**, 354 (1981).
- [34] L.S. Ornstein and F. Zernike, *Proc. K. Ned. Akad. Wet.* **17**, 793 (1914).
- [35] C. Oelschlaeger, G. Waton, E. Buhler, S.J. Candau, and M.E. Cates, *Langmuir* **18**, 3076 (2002).
- [36] F. Kern, F. Lequeux, R. Zana, and S.J. Candau, *Langmuir* **10**, 1714 (1994).
- [37] A.C. Maggs, *Phys. Rev. E* **57**, 2091 (1998).
- [38] B. Hinner, M. Tempel, E. Sackmann, K. Kroy, and E. Frey, *Phys. Rev. Lett.* **81**, 2614 (1998).
- [39] D.C. Morse, *Phys. Rev. E* **58**, R1237 (1998).
- [40] E. Donath, A. Krabi, M. Nirschl, V.M. Shilov, M.I. Zharkikh, and B. Vincent, *J. Chem. Soc., Faraday Trans.* **93**, 115 (1997).
- [41] G.J. Fleer, M.A. Cohen Stuart, J.M.H.M. Scheutjens, T. Cosgrove, and B. Vincent, *Polymers at Interfaces* (Chapman and Hall, London, 1993).
- [42] A.J. Levine and T.C. Lubensky, *Phys. Rev. E* **65**, 011501 (2002).